DOI: 10.1002/adma.200700079

Synthesis and Surface Engineering of Complex Nanostructures by Atomic Layer Deposition**

By *Mato Knez*,* *Kornelius Nielsch*, and *Lauri Niinistö*

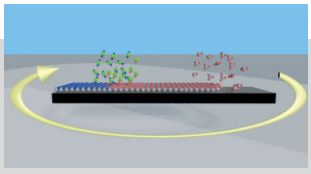

Atomic layer deposition (ALD) has recently become the method of choice for the semiconductor industry to conformally process extremely thin insulating layers (high-k oxides) onto large-area silicon substrates. ALD is also a key technology for the surface modification of complex nanostructured materials. After briefly introducing ALD, this Review will focus on the various aspects of nanomaterials and their processing by ALD, including nanopores, nanowires and -tubes, nanopatterning and nanolaminates as well as low-temperature ALD for organic nanostructures and biomaterials. Finally, selected examples will be given of device applications, illustrating recent innovative approaches of how ALD can be used in nanotechnology.

1. Introduction to ALD and Its Applications in Nanotechnology

Atomic layer deposition (ALD), originally called Atomic layer epitaxy (ALE), was developed in the 1970s by Suntola and Antson to meet the needs of producing high-quality, large-area flat panel displays based on thin film electroluminescence (TFEL).[1] ALD is based on successive, surface-controlled reactions from the gas phase to produce thin films and overlayers in the nanometer range with perfect conformality and process controllability. The principle of ALD is schematically shown in Figure 1 where the thin film growth cycle for a binary compound (TiO_2) from gaseous precursors ($TiCl_4$ and H_2O) is presented as an example.

The TFEL flat panel displays, produced on an industrial scale since 1983, consist of a stack of thin film layers on a glass substrate through which the display is viewed. In the simplest case (a monochromatic yellow-emitting display) the TFEL structure contains a semiconducting light-emitting core (Mn-doped ZnS) surrounded by dielectric layers (Al-Ti-oxide, ATO). In addition, a transparent front electrode (In-Sn-oxide, ITO) and a back electrode (Al) are needed together with passivation and ion barrier layers. As the layer thicknesses are typically in the range of 150–500 nm each, the total thickness of the structure exceeds 1500 nm. The multi- and full color displays have even more complex structures and often involve co-doping. Nevertheless all layers, except for the Al back electrode, can be deposited and doped by ALD.[2]

The processing of TFEL displays by ALD illustrates the advantages of this technique compared to CVD and PLD, for instance. ALD can provide a simple and accurate thickness control as it can be controlled with every cycle. Furthermore, ALD offers facile doping, large area uniformity and thus

[*] Dr. M. Knez, Prof. K. Nielsch
Max Planck Institute of Microstructure Physics
Weinberg 2, 06120 Halle (Germany)
E-mail: ald@mpi-halle.eu
Prof. K. Nielsch
Institute of Applied Physics, University of Hamburg
Jungiusstr. 11, 20335 Hamburg (Germany)
Prof. L. Niinistö
Laboratory of Inorganic and Analytical Chemistry
Helsinki University of Technology
P.O. Box 6100, 02015 Helsinki (Finland)

[**] The authors of this article want to thank the authors of the reprinted images for their kind assistance in providing the original images and Prof. U. Gösele for his valuable comments. L.N. gratefully acknowledges the financial support by the Max-Planck-Institute of Microstructure Physics during his stay in Halle. M.K. and K.N. gratefully acknowledge the financial support by the German Federal Ministry of Education and Research (BMBF) via contract number FKZ 03X5507 and FKZ 03N8701, respectively.

straightforward scale-up. The films exhibit excellent conformality and are dense and pinhole-free. The reactant flux does not need to be controlled as the process is surface-controlled.

In addition to the industrial processing of TFEL displays, ALD has been successfully applied to the depositing of oxide materials including high-*k* insulators[3,4] and other ultrathin metal-oxide films for device applications.[5] A broad overview of successfully deposited materials and the deposition conditions have been given by Puurunen[6] and Kim.[7] Among them the currently mostly investigated materials are, e.g., HfO_2 for electronic applications, but also other metal oxides and nitrides like ZnO, TiO_2, WN_x, or Al_2O_3 because of their electrical or mechanical properties. Apart from those materials a considerable interest can be seen for deposition processes of metals for applications as electrode materials. Here, several groups developed processes for the deposition of Pt, Ru, or Ta.[6]

Besides these applications, the unique potential of ALD for processing nanostructured materials, in general, has been appreciated.[8] The most important large-scale industrial applica-

Dr. Mato Knez was born in 1971 in Augsburg, Germany. He studied chemistry at the University of Ulm (1993–1998) and did his diploma thesis on the synthesis, characterization and theoretical modeling of carbocations. During his doctoral research at the Max-Planck-Institute of Solid State Research in Stuttgart (2000–2003) he investigated the application of plant viruses as templates for the synthesis for novel nanostructures. Subsequently he received his doctoral degree from the University of Ulm. From December 2003 he worked as a post-doctoral researcher at the Max-Planck-Institute of Microstructure Physics in Halle on the application of Atomic Layer Deposition in Nanotechnology. Since November 2006 he is leader of a nanotechnology research group funded by the German Federal Ministry of Education and Research (BMBF) on Functional Nanostructures by Atomic Layer Deposition at the Max-Planck-Institute in Halle.

Prof. Kornelius Nielsch was born in Hamburg, Germany in 1973. He studied physics at the Mercator University in Duisburg (1993–97) and conducted his diploma work on the aerosol synthesis of semiconductor nanoparticles at the University of Lund, Sweden. Subsequently, his doctoral studies on template-based ferromagnetic nanowire arrays were carried out at the Max-Planck-Institute of Microstructure Physics in Halle, Germany. In 2002 he received his doctoral degree with distinction from the Martin-Luther-University Halle–Wittenberg. From October 2002 he worked as a postdoctoral associate at the Massachusetts Institute of Technology, Cambridge, USA. Since October 2003 he is leader of a nanotechnology research group funded by the German Federal Ministry of Education and Research (BMBF) on Multifunctional Nanowires and Nanotubes at the Max-Planck-Institute in Halle. He has co-authored more than 65 refereed journal publications and 3 patents. In 2006 the University of Hamburg has appointed him as a W2 Professor (Associate Professor) for Experimental Physics. Also in 2006, the State of Saxony-Anhalt awarded him the State Research Prize for Basic Research. Since May 2007 he is working as professor at the Institute of Applied Physics in Hamburg.

Prof. Lauri Niinistö was born in Helsinki, Finland, in 1941. He received his M.Sc. and D.Techn. degrees from Helsinki University of Technology in 1968 and 1973, respectively. His doctoral research on the synthesis and crystal structures of metal sulfates and sulfites was partly conducted at the University of Stockholm in 1971–1972. Since 1977 he has been Professor of Inorganic Chemistry at TKK but also worked in France, USA, Austria, and Hungary. His current research is focused on the preparation and characterization of thin films for optoelectronic and electronic devices. He is the author or co-author of more than 400 original publications and reviews. He has received several international honors, among them the Cannizzaro gold medal of the Italian Chemical Society (1996), the FECS award (2000), and honorary doctorates from Tallinn (1990) and Budapest (2002).

ADVANCED MATERIALS

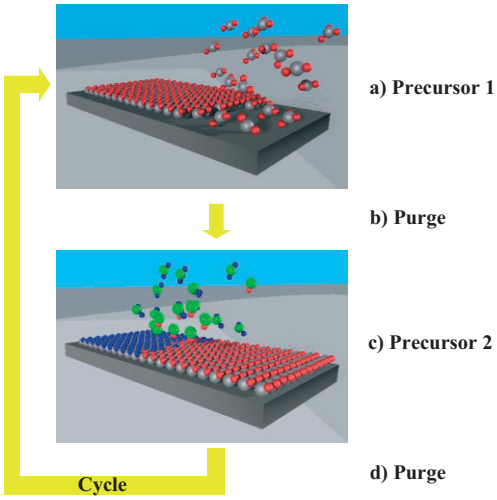

Figure 1. Schematic of an ALD process. The gas flow is indicated with the white arrow. One ALD cycle consists of four separate steps. In step a) the substrate is exposed to precursor molecules (precursor 1) which adsorb ideally as a monolayer on the surface. In step b) the excess of precursor 1 in the gas phase is removed by inert gas purging. In step c) the substrate is exposed to precursor 2 which reacts with the adsorbed precursor 1 to form a layer of the desired material. In step d) the excess of precursor 2 and the reaction by-products are removed by purging. This cycle is repeated (yellow arrow) until the desired thickness of the deposit is obtained.

tion, however, has recently emerged in the semiconductor industry where ALD has been considered as the technique to deposit very thin, highly insulating (high-*k*) oxides to serve as gate dielectrics in MOSFETs and as dielectrics in the trench capacitor structures. As the trench aspect ratio is expected to increase up to 80:1 by the year 2007, ALD is probably the only viable technique for such depositions.[9]

Recently, ALD has attracted the attention of researchers in nanotechnology. The precise control of the deposited layer thickness allows for new strategies in the modification of chemical and physical properties of nanoscaled materials and synthesis routes to novel nanostructures. This review will give an overview of the recently evolved work on the applications of ALD in nanotechnology. The focus is on areas in which the special features of ALD can be exploited, namely the modification or functionalization of existing organic and inorganic nanostructures, the construction of optical devices, like photonic crystals or solar cells, or nanostructures for future electronic devices.

2. Tuning of Nanopores and Porous Materials

Porous materials, particularly with one-dimensional high aspect ratio pores, are of major interest as templates for the synthesis of nanowires and nanotubes. The unique potential of ALD for depositions into nanopores and trenches has been realized since the demonstration of SnO_2 coating of porous silicon with an aspect ratio (AR) of 1:140.[10] Gordon et al.[11] presented a simple kinetic model for step coverage by ALD and also experimentally tested it for the deposition of HfO_2 in narrow holes with AR = 43. However, the pore size of macroporous silicon is comparatively large. The potential of ALD to coat narrow pores becomes obvious if, e.g., mesoporous silicon is used as template. In a recent work, various metal oxides from W, V, Mo, and Ti were deposited on such materials.[12]

Highly uniform nanoporous anodic alumina (AA) can be used as a nanoscale template to test the ALD coating both in practice and theory.[13] ZnO deposition into ultrahigh-aspect-ratio (AR = 5000) nanopores of AA was experimentally demonstrated and modeled with Monte Carlo simulations which predicted that the diffusion-limited coating process would become reaction-limited. Recently, the same group deposited ZnO also on ultra-low density nanoporous silica aerogel monoliths with an effective AR around 100 000 (defined as the ratio of the monolith thickness to average pore size).[14] Even the deposition of metals (W and Ru) on highly porous aerogels to obtain a very high metal surface area was successfully performed.[15,16]

Dense, aligned and uniform arrays of TiO_2 nanotubes were fabricated by ALD with the $TiCl_4/H_2O$ process on nanoporous Al_20_3 templates on a silicon substrate (Fig. 2).[17] The alumina template was then chemically removed to reveal nanotubes with perfectly controllable tube diameter, spacing and wall thickness. In a similar manner ZnO-nanowires were produced by ALD deposition onto a porous alumina template[18] or the pore sizes were reduced by ALD in order to control the thickness of nanowires produced by successive electrochemical deposition.[19] Very recently the group of M. Leskelä demonstrated the photocatalytic properties of such TiO_2-membranes.[20]

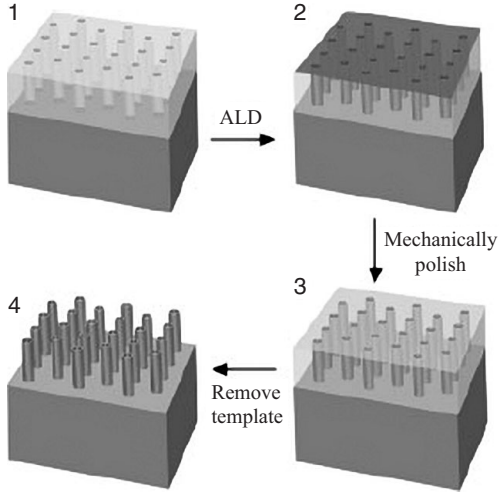

Figure 2. Schematic of the process to create titania nanotube arrays on substrates. 1) Nanoporous-alumina template on a substrate created by anodization of Al film. 2) TiO_2 deposited onto the surface of the template by ALD. 3) Top layer of TiO_2 on alumina removed by gentle mechanical polish. 4) Alumina template chemically etched away to reveal array of titania nanotubes on the substrate. Reproduced with permission from [17].

Other oxide materials fabricated as nanotubes by ALD include TiO_2 and ZrO_2.[21] In this work a commercially available polycarbonate (PC) filter was used as template (AR = 60:1) to be chemically etched away after the ALD deposition at 140 °C. The free-standing nanotubes with ca. 30–200 nm diameters could be fabricated in a one-step process because microcontact printed OTS-SAMs prevented deposition onto both sides of the PC template. These authors also exploited the gas sensing properties of these metal oxide nanotubes. Nb_2O_5 nanotubes have been synthesized in porous anodic alumina templates by an ALD process based on NbI_5 and oxygen by a Swedish group.[22] Niobium oxide (Nb_2O_5) exhibits both electrochromism and catalytic activities.

Furthermore, the honeycomb-like alumina pore structures have been also coated by metallic materials. Most processes for transition metals, like, e.g., Cu, Ni, and Co, based on the reactions of H_2 and organometallic precursors proceed rather slowly (0.03–0.2 Å/cycle).[23] Johansson et al.[24] have employed a three-step ALD process. First, the nanopores are exposed to the copper chloride (CuCl). After the removal of the excess precursor molecules, the chemisorbed molecules on the pore walls are exposed to water and form Cu_2O. In the final step of the ALD cycle the sub-monolayer of metal oxide is transformed into a pure metallic layer by a hydrogen pulse. The three-step process yields a granular and discontinuous metallic film on the pore walls. This three-step ALD process was originally introduced by Utriainen et al.[25] who processed Ni films by first depositing NiO and then reducing it by H_2. A more direct approach is also possible when the metal beta-diketonate precursor $M(acac)_2$ (M = Ni, Cu, Pt) is chemisorbed onto the substrate and then reduced by H_2 in the same ALD cycle.[25] Daub et al.[26] applied a very similar three-step ALD process based on $NiCp_2$ (Nickelocene) and $CoCp_2$ (Cobaltocene) for the synthesis of nickel and cobalt nanotubes in porous alumina membranes and obtained quite granular metal films. Alternatively, they tried the deposition of nickel and cobalt oxide by using the same precursors and ozone pulses. After the ALD process, the transition metal oxide tubes were reduced in hydrogen at elevated temperatures. The resulting ferromagnetic nanotubes exhibited significantly improved magnetic properties, a preferential magnetization direction along the tube axis, a very fine granular crystal structure and a low degree of surface roughness. The reduction of atomic layer deposited metal oxides or nitrides seems to be a very promising approach for the formation of continuous transition metal films on complex surfaces. This process has also been successfully applied on atomic layer deposited copper nitride films in high aspect ration silicon trenches by the Gordon group.[27]

ALD can also be used to fine-tune the surface properties and diameters of nanopores to achieve functional nanopore detectors.[28] Using 5 cycles of the well-established alumina ALD process from TMA and water, a 2 nm diameter ion-beam sculpted nanopore could be reproducibly adjusted down to 1 nm diameter, with an error of only ±0.12 nm.

3. VLS Growth of Semiconductor Nanowires

The synthesis of semiconductor nanowires NWs is currently very intensively studied[29] by means of pulsed laser deposition (PLD), molecular beam epitaxy (MBE) and chemical vapor deposition (CVD). Most semiconducting materials, e.g., Si, Ge, ZnO, and GaAs have been realized by this approach and published in several hundred papers each year. The growth of multilayer nanowires with atomic resolution at the interfaces is challenging and for certain material systems, e.g., InP/InAs, high-resolution multilayer nanowires have been successfully synthesized.[30] In combination with ALD a better control of VLS growth for binary semiconductor nanowires for a broader range of materials could be provided.

The processing of both II-VI and III-V semiconductor nanowires by ALD has been successfully demonstrated. The Vapor–Liquid–Solid (VLS) growth has been used to initiate ALD of single crystalline nanowires consisting of alternating layers of ZnSe and CdSe which form a superlattice (Fig. 3)[31] while a pulsed MOCVD process has been used to deposit GaN.[32] Because of the strict separation of the precursor pulses (trimethylgallium and ammonia) the latter process by its nature appears to represent essentially ALD.

Another recent example of employing ALD for the growth of nanowires is the formation of KCl NWs by a rather unusual two-step process where at first tantalum oxide is formed inside microchannel glass by a conventional ALD reaction from $TaCl_5$ and H_2O. In the next stage, the hydrogen chloride released in the ALD reaction etches K_2O from the glass substrate whereupon forming KCl and water. The final phase in this process chain involves the nucleation of KCl on the microchannel walls to form KCl nanowires. The aspect ratio of the nanowires is about 10 to 100. They span the entire length of the 5 μm channels and the NW diameter ranges from 50 to 700 nm.[33]

There should not be any fundamental reason that the ALD growth of semiconductor NWs should be limited to these few examples. It can most probably be extended to other binary semiconductors. The research activity in this area is likely to increase rapidly in the very near future.

4. Conformal Coating of CNTs and Semiconductor Nanowires

The surface-controlled nature of ALD can be exploited to an extreme when nanotubes and nanowires are coated to achieve the desired materials properties for functional device applications. Thus, carbon nanotubes (CNTs) possessing a well defined molecular and nanoscale hollow tubular structure can be functionalized as such by ALD coatings[34,35] or used as templates for nanotubes of various inorganic oxides such as ruthenium oxide.[36] Suspended single-walled carbon nanotubes are known to be chemically inert to ALD precursor molecules but nevertheless they can be conformally ALD-

ADVANCED MATERIALS

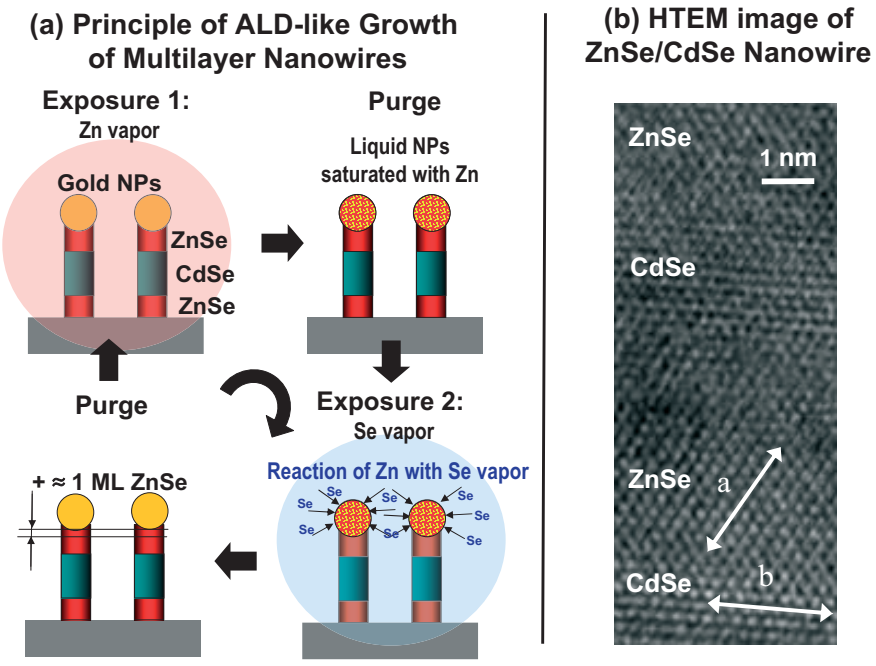

Figure 3. a) The principle of ALD-like growth of binary semiconductor nanowires under Vapour Liquid Solid (VLS) growth conditions. *(Interpretation by the review authors)*: *Exposure 1:* The sample is exposed to Zn (or Cd) vapor and these elements are dissolved in the liquid gold nanoparticle until the saturation solubility is reached. *Purge:* Removal of the Zn (or Cd) vapor from the reaction chamber. *Exposure 2:* The Zn (or Cd) atoms in the gold droplets are reacting with Se vapor; ZnSe (or CdSe) is formed and precipitated in the solid phase on the nanowire top. Finally, the Se vapor is removed from the reaction chamber by the *second purge*. In contrast to conventional ALD, where the deposition process is surface limited and the precursor molecules are adsorbed on the sample surface, here in the VLS growth process for nanowires by Solanki et al the amount of deposited semiconductor material per cycle is depending on the solubility of Zn or Cd in the liquid gold nanoparticles and the nanoparticle volume. By each ALD-like cycle approximately 1 monolayer of ZnSe or CdSe has been deposited. b) HRTEM image showing ZnSe/CdSe superlattice nanowire. The inserted arrows indicate the direction of (111) planes of ZnSe(a) and CdSe(b). The scale bar is 1 nm. Reproduced with permission from [31]. Copyright 2002 American Institute of Physics.

coated by Al_2O_3 or HfO_2 if first functionalized by attaching $-NO_2$ groups to the sidewalls.[37]

The renewed interest in germanium as a material-of-choice for future electronics, potentially replacing silicon, has initiated some recent research also involving ALD. Thus, Wang Chang et al.[38] reported on the surface chemistry and electrical properties of germanium nanowires (GeNWs) where the high-*k* dielectric HfO_2 was grown onto the GeNW surfaces by ALD.

A unique ALD route to monocrystalline spinel nanotubes was recently reported by Fan et al.[39] who exploited the Kirkendall effect to fabricate nanotubes (Fig. 4). Here the ZnO nanowires were conformally coated with ALD alumina using trimethylaluminium (TMA) and water at 200 °C whereafter an interfacial solid-state reaction at an elevated annealing temperature of 700 °C consumed the ZnO core, producing a hollow ultralong spinel $ZnAlO_4$ nanotube with a diameter of 40 nm and wall thickness of 10 nm. A similar approach to produce $MgAl_2O_4$ spinel nanotubes was performed with Al_2O_3-coated MgO nanowires, however, not involving the Kirkendall effect.[40]

The wide-gap semiconductor ZnO nanowires or nanorods can be conformally ALD-coated with Al_2O_3.[41,42] ALD can also be employed to initiate the growth of ZnO nanowires. ZnO nanobridge devices for gas and UV sensing were integrated on the silicon-on-insulator substrates based on this approach.[43]

Another wide-gap semiconductor, namely GaN, can be grown in the form of nanowires which have attracted much attention for the fabrication of nanometer-sized high-power electronic and blue-light-emitting optoelectronic devices.[44] The role of ALD in these devices is to conformally deposit a 10–20 nm shell of amorphous alumina as a passivation layer around the 50 nm thick GaN nanowires.[45]

5. Area-Selective ALD and Nanopatterning

Although the ALD usually covers all accessible surfaces in the reactor, it is possible to perform area-selective deposition and nanoscaled patterning of surfaces. To obtain such patterns there are two principal ways, both of which are relying on lithographical processes, like conventional lithography or microcontact printing. One approach is patterning the substrate with overcoatings of a (mostly polymeric) resist layer in order to protect the underlying surface. After an ALD deposition, a lift-off process can be performed to selectively remove the unwanted areas.[46–48]

In a common lithographic procedure, Biercuk et al.[46] placed a film of photoresist or PMMA on a Si wafer and exposed it through a photomask or wrote a pattern onto it with an electron beam. After ALD deposition of HfO_2, ZrO_2, or Al_2O_3, the entire surface was covered with an oxide overlayer. A lift-off process lead to a patterned Si wafer with highly controllable film thickness in the range of 2.5–100 nm. Park et al.[47] fabricated TiO_2 patterns by light-stamping lithography (LSL). This process is similar to microcontact printing (μCP), however, not transferring molecular ink adsorbed to the stamp but instead depositing a pattern of PDMS from the stamp itself by abrasive (soft) imprint lithography. This method was used to produce both positive and negative TiO_2 patterns. Positive tone pattern is achieved by placing a PDMS stamp on a substrate and irradiating with UV light through

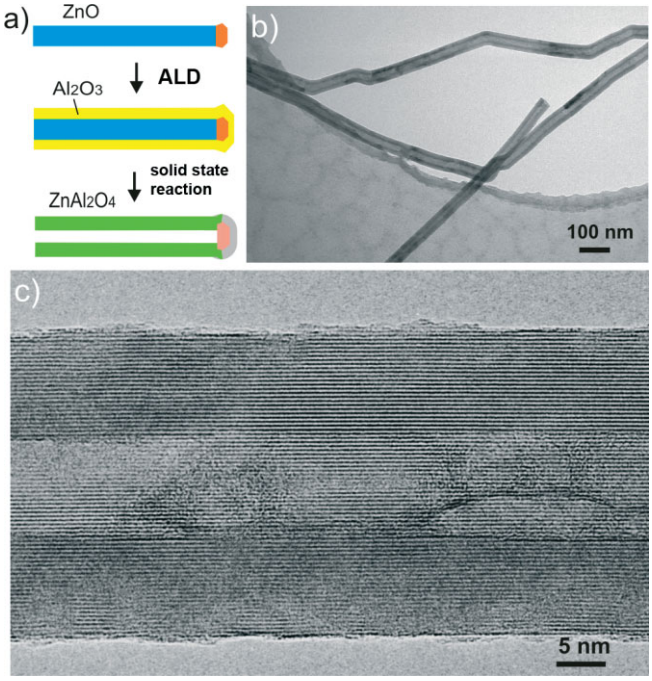

Figure 4. Schematics of the formation process of $ZnAl_2O_4$ spinel nanotubes. a) Single crystal ZnO nanowires are grown via the vapor-liquid-solid mechanism using Au nanoparticles as catalyst. b) The nanowires are coated with a uniform layer of Al_2O_3 by atomic layer deposition, forming core–shell ZnO-Al_2O_3 nanowires. c) Annealing the core–shell nanowires leads to the formation of $ZnAl_2O_4$ nanotubes via a spinel-forming interfacial solid-state reaction involving the Kirkendall effect. Reproduced with permission from [39]. Copyright 2006 Nature Publishing Group.

the polymeric master. The PDMS in the contact area is bonded to the substrate and after mechanical removal of the master, PDMS remains in the initial contact areas. For the negative tone pattern, a layer of TiO_2 is deposited by ALD on the substrate. After removal of the PDMS master and chemical etching, a TiO_2 pattern remains on the substrate (Fig. 5). Alternatively, the substrate is covered with a TiO_2-layer and afterwards treated by LSL, which then, after the lift-off process, leads to a positive pattern. Although this method was demonstrated for TiO_2 only, it is expected that it will work in a similar manner for a number of other materials, too.

A different patterning approach via ALD is the passivation of surface areas by immobilizing molecules which hinder the ALD precursor molecules to attach.[48–52] In those cases, a separate lift-off process is not required. The driving force for the inhibition of ALD deposition in selected areas is the repulsive force between the deposited monolayers of molecules and the precursor molecules approaching from the gas phase. In most cases, the selectivity arises from polar and non-polar molecules building a pattern on the substrate. A commonly used technique to produce such a molecular pattern is soft-imprint-lithography. For this purpose, a patterned polymer master was inked with molecules prior to the contact with the substrate. The molecules adsorb locally on the substrate and thus change the chemical environment. If both the monolayer and the ALD precursor molecules are polar, no ALD deposition in those areas is expected. The work of Seo et al.[48] shows patterning of gold with non-polar thiol-monolayers and successive immobilization of a polar self-assembled thiol monolayer in the remaining area. An ALD deposition of TiO_2 took selectively place in the area of polar molecules. A similar approach was performed by Park et al.,[49] but they applied non-polar silane monolayers to inhibit the ALD deposition of Ru.

Apart from the patterning of surfaces by μCP there are also other lithography based methods for pattern selective ALD. In the work of Lee et al.,[50] a monolayer of non-polar silane molecules was adsorbed on a silicon wafer and subsequently locally oxidized. For this purpose, a patterned TiO_2-stamp was contacted with the substrate and irradiated with UV light. In the contact area of the TiO_2 and the silane molecules, the monolayer was decomposed leaving an oxidized silicon surface for the local ALD deposition of ZrO_2. In this case the authors were able to grow area-selective ZrO_2 up to a thickness of 15 nm.

Chen et al.[51,52] produced first a silicon wafer with a pattern of hydrogen- and hydroxo-terminated silicon and successively bound monolayers of ALD-inhibiting molecules onto either of those two surface areas (Fig. 6). Successively they selectively deposited HfO_2 and Pt in a controlled way by ALD. An area-selectivity of ALD deposition can also be introduced by prepatterning of substrates with metals. In the work of Whitney et al.[53] glass and Si surfaces were patterned with triangular Ag nanoparticles by nanosphere lithography. The successive deposition of Al_2O_3 by ALD was selective to the Ag nanoparticles.

The group of Summers[54,55] used a substrate patterned with a self-assembled monolayer of hexagonally arranged polystyrene and SiO_2 nanospheres. The substrate was processed by ALD to deposit TiO_2, Al_2O_3, or ZnS onto it.[54,55] After removal of the top layer of TiO_2 with an ion beam followed by a removal of the polymer beads, a micrometer-scaled surface with TiO_2-nanobowls was obtained (Fig. 7). In this particular process, the ALD method could show its major advantage, compared to other deposition methods like CVD or PLD, in terms of conformal coatings. The hollow area between the nanospheres can easily be accessed by the precursor and the "hidden" surface area thus conformally covered. Other gas-phase deposition methods, being basically line-of-sight techniques, do not offer this possibility making ALD the method-of-choice for the deposition onto complex, hollow substrates.

ALD also enables to deposit a very controlled layer thickness even on highly complex-shaped substrates, like monolayers of polymer nanospheres. ALD deposition on patterns of organic monolayers as compared to the lift-off strategies is easier to perform. Here the temperature does not play such an essential role, since most of the molecules used can resist even much higher temperatures (up to several hundred degrees Celsius) than polymers. The advantage is obvious, as this method can be applied to most materials which can be depos-

ADVANCED MATERIALS

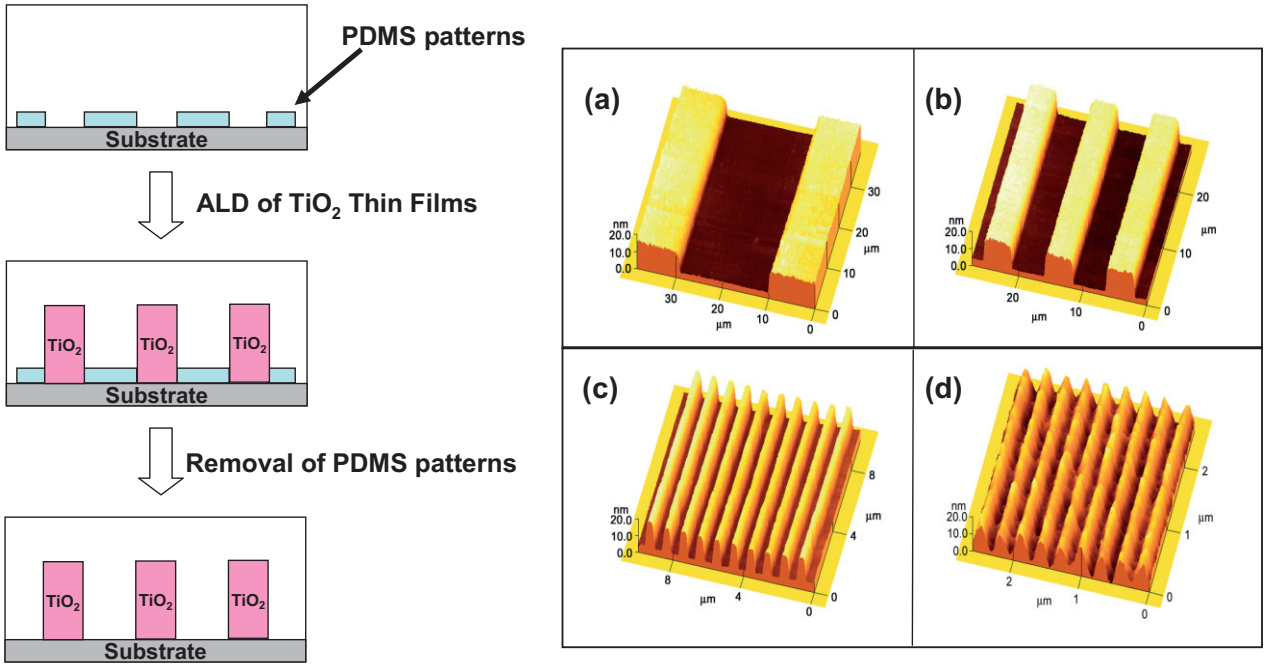

Figure 5. Left: Schematic outline of the procedure to fabricate patterned TiO_2 thin films by using selective ALD on PDMS-patterned Si substrates. Right: AFM images of the patterned TiO_2 thin films created by selective ALD on PDMS-patterned Si substrates. Reproduced with permission from [47]. Copyright 2006 American Chemical Society.

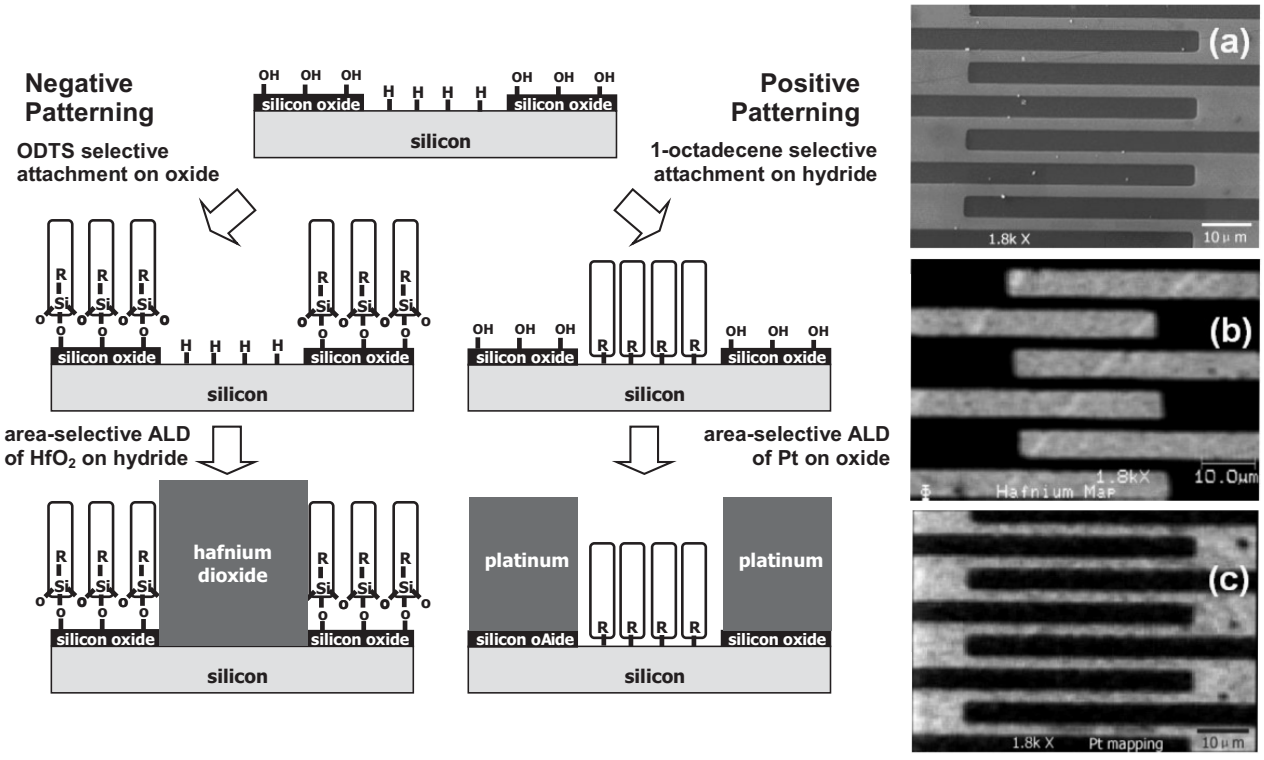

Figure 6. Left: Schematic illustration of two area-selective ALD schemes made possible through selective surface modifications. Right: a) SEM image of a test structure; the brighter pattern in this image shows the thermal oxide region, the darker area is the Si-H region. b) AES elemental mapping of the test structure after negative patterning and HfO_2 deposition by ALD on the Si-H region (according to the left-handed route in the schematic). c) AES elemental mapping of the test structure after positive patterning and Pt deposition by ALD on the oxide region (according to the right handed route in the schematic). Reproduced with permission from [52].

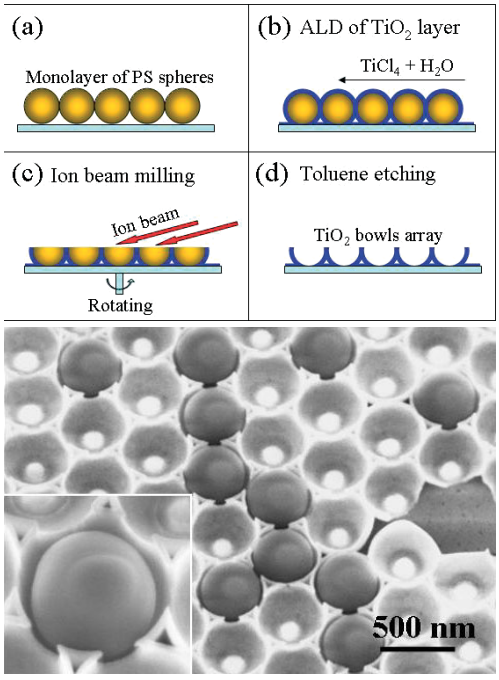

Figure 7. Upper image: Schematic of the synthesis strategy for TiO_2 nano-bowl arrays. Lower image: Polystyrene (PS) spheres lying on the top of a TiO_2 nano-bowls array after applying a drop of PS spheres and washing with ethanol. The insert shows a 450 nm PS sphere confined inside a TiO_2 nano-bowl. Reproduced with permission from [54]. Copyright 2004 American Chemical Society.

ited by ALD. However, a significant disadvantage is the two-dimensionality of the deposition. In most cases, if surfaces are patterned by organic molecules, the patterning relies on very flat substrates. Probably in future experiments, a combination of both strategies with an ALD process could lead to a new kind of patterned structures, maybe even in 3D.

6. Low-Temperature ALD for Organic Nanostructures and Biomaterials

Although ALD is mainly applied to substrates which can easily resist elevated or even high temperatures (in the range of 100–500 °C, or above), there is a growing interest in ALD at lower temperatures (up to 100 °C) or even at room temperature (RT).

Polymers have nowadays become an increasingly important group of materials. Starting from packaging materials for food and other goods to computer cases or automobile parts or even building blocks for nanostructuring, polymers show universal usability. The biggest advantage of the polymers is their formability to all kinds of shapes and structures. However, a major disadvantage is the sensitivity to high temperatures which most polymers exhibit. With low-temperature ALD (LT-ALD) it has finally become possible to conformally coat polymers with materials which could not be deposited onto temperature-sensitive polymers before. However, the growth mechanism in LT-ALD differs somewhat from the one prevailing at higher temperatures. In particular with Al_2O_3-deposition enhanced growth rates can be frequently observed. Thus, the group of S. M. George[56,57] have recently considered the nucleation and growth of Al_2O_3 on polymers. Although the mechanism is not yet completely understood, it seems that particularly for polymers a certain solubility of TMA during the first pulses can be taken into account, which leads to an increased growth rate of Al_2O_3 during the first cycles. However, this model cannot explain the differences in growth rate if other substrates than polymers are used. Future experiments should lead to a deeper insight into this special topic and probably to some universal model.

The first successful experiments to perform ALD at room temperature were published already in 1994 by Gasser et al.[58] depositing SiO_2 from $Si(NCO)_4$ and water. Later in 1997 Klaus et al.[59] applied LT-ALD to deposit SiO_2 from $SiCl_4$ and water; however, this reaction required a catalyst, since the reactivity of the precursors was otherwise too low. For this reaction, the required temperature is higher than 300 °C, but by adding pyridine as catalyst to the reaction (Fig. 8) the reaction temperature was lowered to 300 K. At about the same time, Luo et al.[60] showed that even without catalysts, an ALD process can be performed at room temperature. In a UHV chamber they epitaxially deposited CdS on a ZnSe crystal, thus obtaining a II-VI semiconductor. Although in those cases a LT-ALD deposition does not show any essential advantages as compared to the high-temperature depositions, the follow-up experiments made it clear that LT-ALD is of particular interest for the coating of polymers.

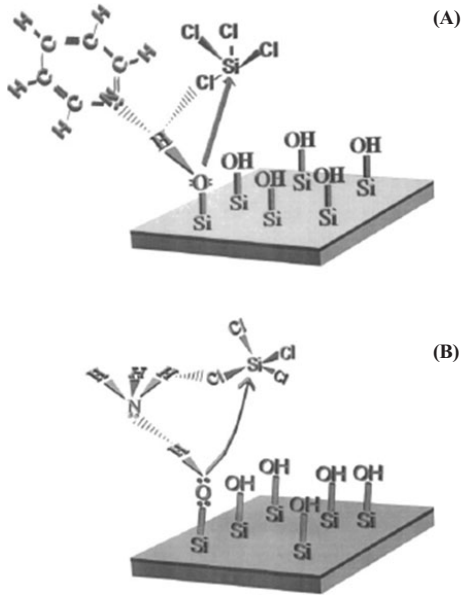

Figure 8. Proposed mechanism for Lewis base catalysis of SiO_2 atomic layer deposition during the $SiCl_4$ half-reaction using: A) pyridine; and B) NH_3. Reproduced with permission from [68]. Copyright 2000 Elsevier.

ADVANCED MATERIALS

In an interesting recent experiment, Groner et al.[61] managed to deposit Al_2O_3 on a PET bottle at 58 °C. Although the purpose of the experiment might be questionable in the first place, there is a reasonable background for it as in the case of, e.g., food packaging, the coating by ALD might slow down the diffusion of gas through the polymer and thus extend the shelf life of the products.

In the same year, Ferguson et al.[62] encapsulated polyethylene particles in Al_2O_3. The reaction temperature was higher than RT (77 °C), but it was still below the melting temperature of polythylene (105–115 °C). Some follow-up experiments showed that a variety of polymer materials like PS and PVA can be used as templates in an analogue way.[63,64] The advantage of ALD for the encapsulation of polymer nanoparticles is obvious: The control of the film thickness and the quality of the deposited films are higher than those achieved by other deposition methods.

LT-ALD also enables the coating of biomolecules with thin films. This topic may become interesting in future, since a number of biological structures show interesting effects because of their naturally appearing nano- and microstructures. Here, for instance the well-known lotus leaf can be mentioned, which shows highly hydrophobic behavior due to its nanostructures. Other examples are, e.g., the colorful butterfly wings or the sticky feet from geckos, which enables those animals to easily climb up walls. In some cases those effects in nature cannot easily be artificially reproduced. The ALD could enable an easy and accurate replication of such structures for a possible commercial use. First experiments of such kind involved the deposition of Al_2O_3 and TiO_2 on tobacco mosaic virus (TMV) (Fig. 9) and on protein spheres (ferritin).[65] Those molecules are even more temperature-sensitive than most polymers and require deposition temperatures of less than 60–80 °C. Recently, butterfly wings were covered by ALD, thus replicating their highly complex morphology (Fig. 10).[66] Potentially, novel optically active structures can be synthesized by this ALD replication technique of nanostructured biomaterials. For instance the mentioned replication of the butterfly wing structure showed expectedly interesting coloration. Further modification of such structures by ALD could improve their tunability and possibly lead to new approaches for optical elements, e.g., in holography.

Recently, TiO_2 was deposited onto cellulose fibers from filter paper.[67] This was, however, done at a comparatively high

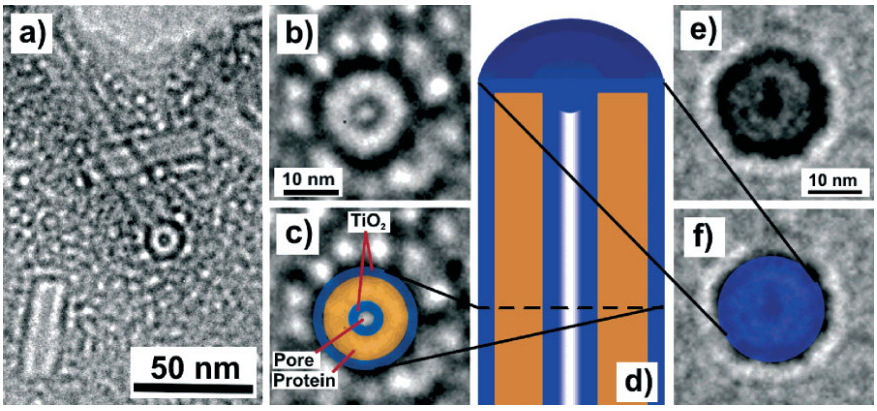

Figure 9. Image a: TEM (200 kV) image of TMV treated with TiO_2 by ALD. A disk from destroyed TMV (circular particle) embedded in an amorphous TiO_2-film can be seen in the cross-sectional view. TiO_2 covering the interior channel appears to be hollow with a pore diameter of 1–1.5 nm and a wall thickness of 1 nm. The covered inner channel of the viruses appears brighter along the axis, confirming the assumption of a hollow TiO_2 nanotube. Image b: Further magnification of a TiO_2-covered TMV-disc showing a hollow area inside the TiO_2-covered interior channel of the virus. Image c: Recolored image b). The orange circle represents the viral protein sheath. The blue color shows the TiO_2-coating of viral surface (outer surface and channel surface). The surrounding gray area is the embedding amorphous TiO_2-film. Image d: Sketch of a cross-section of a TiO_2-covered TMV with same colors as in image (c). In the top part of the virus no pore is visible in the center. This part represents the assumed clogged area of the inner viral channel. Image e: Further magnification of a TiO_2-covered TMV-disc showing a clogged interior channel of the virus. Image f: Recolored image e). Reproduced with permission from [65]. Copyright 2006 American Chemical Society.

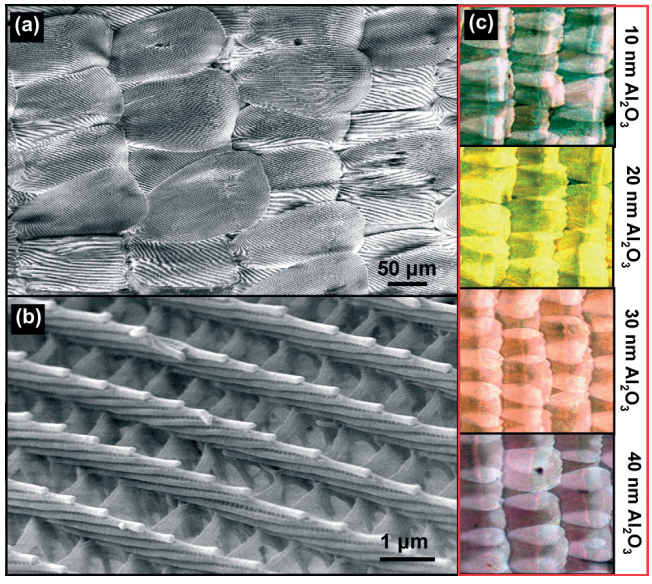

Figure 10. Images of the alumina replicas of the butterfly wing scales. a) A low-magnification SEM image of the alumina replicas of the butterfly wing scales on silicon substrate after the butterfly template was completely removed. b) A higher magnification SEM image of an alumina replicated scale, where the replica exhibits exactly the same fine structures. c) Micrographs of the replicas with varying thickness of deposited Al_2O_3. Reproduced with permission from [66]. Copyright 2006 American Chemical Society.

temperature (150 °C). Nevertheless, the experiments show that there is an increasing interest in the combination of natural materials and a highly surface-controlled deposition technique. More results of similar nature are expected to shortly become available, after these initial steps towards protecting and replicating of biological macromolecules by ALD.

Currently only a few materials have been deposited at low temperatures (i.e., temperatures lower than 100 °C). Apart from SiO_2,[58,59,68] depositions of CdS,[60] Al_2O_3,[61–66] TiO_2,[65,69] B_2O_3,[70] V_2O_5,[71] HfO_2,[46,72] ZrO_2,[46] ZnO[73], and Pd[74,75] have been demonstrated (Table 1). It has become obvious that there is a growing demand for new precursors which would enable the deposition of additional materials at low temperatures. In particular, the deposition of metals would be highly desirable since this would be a good alternative to electrochemistry to introduce new functionalities to temperature-sensitive materials, since with ALD one does not need a conductive substrate. Even with electroless deposition of metals, the ALD might exhibit advantages, since the thickness of the deposited layer can be controlled much more precisely. Together with the possibility to deposit binary materials, like metal oxides or nitrides, the ALD would be much more universal than electrochemical methods.

Table 1. A summary of published low-temperature (≤100 °C) ALD processes.

Material	Temperature	Precursor 1	Precrusor 2	Reference
SiO_2	30°C [a]	$SiCl_4$	H_2O	[68]
	27°C [b]	$SiCl_4$	H_2O	[59]
	RT	$Si(NCO)_4$	H_2O	[58]
CdS	RT	$Cd(Me)_2$	H_2S	[60]
Al_2O_3	33°C, 58°C	TMA	H_2O	[61]
	77°C			[62]
	80°C			[63]
	45°C			[64]
	35°C			[65]
	100°C			[66]
TiO_2	35°C	$Ti(OiPr)_4$	H_2O	[65]
	100°C	$TiCl_4$	H_2O	[69]
B_2O_3	20°C	BBr_3	H_2O	[70]
V_2O_5	90°C	$VO(OiPr)_3$	O_2	[71]
HfO_2	100°C	$Hf[N(Me)_2]_4$	H_2O	[46]
	90°C			[72]
ZrO_2	100°C	$Zr[N(Me)_2]_4$	H_2O	[46]
ZnO	85°C	$ZnEt_2$	H_2O	[73]
Pd	80°C	$Pd(Hfac)_2$	H_2	[74]
	80°C	$Pd(Hfac)_2$	H_2-Plasma	[75]

[a] Catalyzed with NH_3. [b] Catalyzed with pyridine.

7. Photonic Crystals and Optics

In the past decade photonic crystals have been intensively investigated for their potential to confine light as well as to guide light. As optical analogues of semiconductors,[76–78] many optical phenomena of photonic crystals are related to their characteristic photonic bandgap. One of the best established synthetic routes to three-dimensional photonic crystals is replication, infiltration, or coating of synthetic opal structures, formed by self-assembly of spherical polymer or silica micro- and nanoparticles. By conformal nanometer-thin coating of these complex nanostructures with semiconductors or metal-oxides possessing a high refractive index or luminescent properties, the photonic bandgap can be tuned over a wide range.[76,78] Especially for photonic crystals, templated by polymer nanostructures, low-temperature ALD processes are crucial (see Sec. 6).

Several research groups employed chemical vapor deposition (CVD) for the coating or replication of synthetic opals or other 3D photonic crystals.[79–82] In contrast to CVD, atomic layer deposition yields highly conformal film growth with nanometer-scale thickness control and has proven to be an ideal technique for the infiltration of these 3D porous architectures. Furthermore, multilayer coating and doping of the 3D thin film structures can be performed in a very controlled manner. The first report on ALD of opal structures was published in a collaborative paper of the Gordon (Harvard) and Tolbert (University of California, L.A.) groups in 2003.[83] They formed an inverse opal structure of tungsten nitride by ALD infiltration of the so-called 3D colloid crystal and subsequently removed the silica colloid spheres by HF etching. In the same year, King et al.[84,85] reported the synthesis of ZnS inverse opal structures doped with manganese by employing a similar approach. They achieved more than 95 % filling fraction of the semiconductor material in the opal structure and performed the first detailed optical characterizations on photonic crystals processed by ALD. Most recently, this group from Georgia Institute of Technology presented a TiO_2-based 3D-photonic crystal (Fig. 11).[86] This group also demonstrated that the optical spectra of this photonic crystal can be tuned over a wide range by varying the number of ALD cycles (Fig. 11c). They deposited by ALD an additional sacrificial-layer layer of ZnS or Al_2O_3 on the opal structure. This was done before the ALD process to deposit the optically active material (e.g., TiO_2), and in this way they could enhance the variation in the optical properties of the TiO_2 photonic crystal.[55]

More recently, the ALD approach for self-assembled 3D-photonic crystals has been extended to a broad variety of materials, e.g., Ta_3N_5,[87] ZnO,[73,88] GaAs,[89] Al_2O_3,[90] and TiO_2/ZnS[91] to produce multilayer inverse opal structures with a periodicity ranging from 250 to 500 nm. An overview of this very active field of ALD applications in nanotechnology is given in Table 2. Alternatively, ALD has also been employed to infiltrate holographically defined polymer photonic crystal templates.[69] In contrast to the self-assembled synthetic opal structures, these holographic structures exhibit a perfect arrangement in 3D. However, only low temperature ALD processes can be employed to process these nanostructures.

In the field of 2D-photonic crystals only one paper has been published so far.[92] In this work a 2D array of ZnO nanowires

ADVANCED MATERIALS

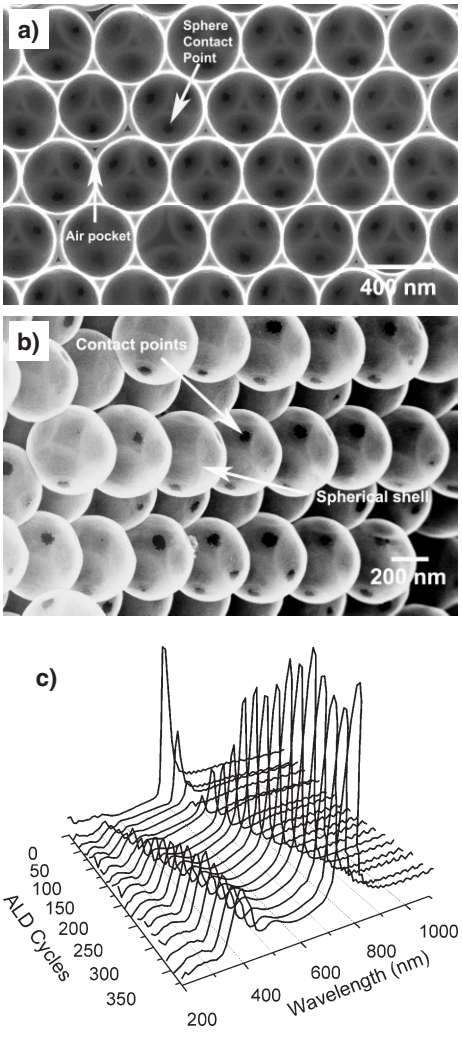

Figure 11. SEM images of a 433 nm TiO_2 inverse opal. a) Ion-milled (111) surface, b) fracture surface. c) Reflectivity data from stepwise TiO_2-infiltrated 266 nm SiO_2 opal. Reproduced with permission from [86].

was coated with thick TiO_2 layer and interconnections were formed between the vertically aligned and close packed ZnO nanowires. In the emerging field of plasmonic nanostructures the tunability of a SERS (Surface Enhanced Raman Scattering) active metallic nanodot arrays by a controlled ALD of Al_2O_3 onto silver dots was demonstrated.[53] This ALD approach is also very promising for the generation of biocompatible coatings on (mostly antibacterial) SERS active nanostructures. The optical activity is reduced exponentially by the transparent oxide coatings, but on the other hand ultra-thin layer can be conformally deposited on these highly textured surfaces in order to optimize the SERS activities and to achieve a bio-compatible surface at the same time.

More conventional optical devices were also synthesized by ALD. The group of S. M. George grew tungsten/alumina nanolaminates by ALD, which have a potential application in X-ray optics.[93,94] The optical properties of the gratings were

Table 2. Template-based synthesis of 3D (and 2D) photonic crystals by atomic layer deposition.

Materials deposited by ALD	Template Structure for Photonic Crystal	Reference
WN	Opal, SiO_2 spheres	[83]
ZnS:Mn (Doping)	Opal, SiO_2 spheres	[84, 85]
TiO_2	Opal, SiO_2 spheres	[86]
TiO_2	Opal, SiO_2 spheres + ZnS or Al_2O_3 sacrificial layer	[55]
Ta_3N_5	Opal, SiO_2 spheres	[87]
ZnO	Opal, polystyrene spheres	[73, 88]
GaAs	Opal, SiO_2 spheres	[89]
Al_2O_3	Opal, SiO_2 spheres	[90]
TiO_2/ZnS multilayer	Opal, SiO_2 spheres	[91]
TiO_2	3D Holographic Polymer Structure	[69]
TiO_2	2D ZnO nanowire array	[92]

tuned by depositing nanolaminates, like TiO_2/SiO_2 or SiO_2/Al_2O_3. J. J. Wang et al.[95] developed a high-performance infrared polarizer and polarizing beam splitter by filling high-aspect ratio trenches (trench depth/width up to 14) with nanolaminates. The refractive index of the filling material in the trenches was varied by the nanolaminate composition.[95] The same group has also realized arrays of nano- and microlenses by a similar approach.[96]

In conclusion, the application of ALD for optical devices is currently one of the most active development fields for ALD. There are undoubtedly numerous new potential applications emerging from fundamental research, especially concerning photonic and plasmonic nanostructures. These should lead to first commercialized ALD products in conventional optics within the next few years.

8. Devices for Advanced Applications by ALD

During the very recent years more and more examples have emerged demonstrating how ALD can be exploited to fabricate nanoscale devices. The role of ALD in the fabrication of nanodevices may, for instance, involve the deposition of a very thin (8 nm) and conformal high-*k* dielectric layer of ZrO_2, necessary for the transistor function of a nanowire field effect transistor (FET) based on single-walled CNTs.[97] Combining carbon SWNTs with ALD-deposited high-*k* HfO_2 has resulted in FETs where the electron transport is nearly ballistic.[98] Most recently, Keem et al.[99] fabricated omega-shaped-gate ZnO nanowire FETs where the wires are ALD-coated by alumina to act not only as gate material but also as a passivation layer.

Another example of combining the unique characteristics of ALD with nanostructures is the processing of a new type of extremely thin absorber (ETA) 3D solar cells where ALD is used to infiltrate p-type $CuInS_2$ inside the pores of nanostructured n-type TiO_2 (Fig. 12). Tuning of the ALD parameters, in order to deposit the ternary semiconductor inside the nanoporous TiO_2 matrix, and then incorporating an In_2S_3 buffer layer by ALD, represents an experimental challenge but

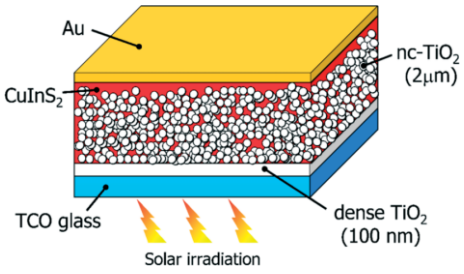

Figure 12. Structure of an inorganic, solid-state 3D solar cell. Reproduced with permission from [100].

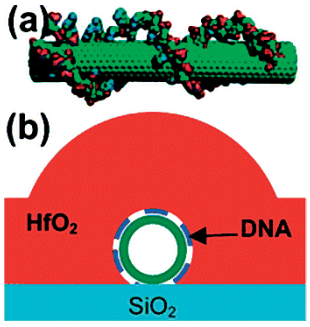

Figure 13. DNA functionalization for nanotube electronics. a) Schematic of a DNA coated SWNT. b) Cross-sectional view of HfO_2 (3 nm by ALD) conformally deposited on a DNA functionalized nanotube lying on a SiO_2 substrate. Reproduced with permission from [72]. Copyright 2006 American Chemical Society.

nevertheless the results already at this early stage of development are very promising.[100] The energy conversion of the solid-state 3D cell (Fig. 12) exceeds 4 % which doubles the previously reported best performance of inorganic ETA cells.

Carbon nanotubes (SWNTs) were adsorbed on top of a 100 nm-thick ALD-grown alumina to form electromechanical transducer elements to act as sensor with the highest reported piezoresistive gauge factor of approximately 210.[101] Alumina by ALD was exploited as tunnel oxide barrier when fabricating single electron memory devices.[102] A nonvolatile memory behavior was observed with each bit represented by about 15 electrons.

Samanta et al.[103] recently exploited ALD for a non-volatile memory application and deposited amorphous hafnium silicate to embed tungsten metal nanocrystals of 5 nm size. Kim Nam et al.[104] likewise recognized the potential of ALD to deposit Zr and Hf high-*k* materials such as silicates and aluminates. They also considered the nonconventional metal alkoxide-based ALD process, which uses no external oxygen source, as first reported by Ritala et al.[105]

While using chemical vapor deposition (CVD) to synthesize single-crystalline germanium NWs (GeNWs), Wang et al.[106] and Wang and Dai[107] fabricated field-effect transistors (FETs) based on GeNWs by growing the thin (12 nm) HfO_2 gate oxide by ALD.

Carbon nanotubes, especially the SWNTs, can be considered as quasi 1D materials suitable for future high-performance electronics.[98] However, the inherent lack of functional groups on nanotubes prevents their conformal and uniform coating by ALD, unless the inner surface is functionalized. Following the pioneering experiments of Hermann et al.[34] as well as those of Farmer and Gordon[37] who attached nitrogroups onto the sidewalls, Lu et al.[72] functionalized the SWNTs by DNA resulting in enhanced nucleation and growth of the high-*k* oxide HfO_2 by ALD at 90 °C (Fig. 13). The thickness limit of the high-*k* insulating oxide can be pushed down to 2–3 nm which makes it possible to approach the ultimate vertical scaling limit of nanotube FETs and reliably achieve $S = 60$ mV/decade, at room temperature.

Another device application is emerging from the use of ALD to deposit WS_2. This process provides the low-friction and low-wear coatings needed for moving mechanical assemblies as required in certain MEMS devices.[108]

Most recent reports on the use of ALD for devices involve the oxides of hafnium, aluminum and iridium. Thus, high-performance thin-film transistors (TFTs) on silicon and flexible plastic substrates are based on networks of SWNTs and high-capacitance bilayer dielectrics which consist of ALD-grown HfO_2 and spin-cast epoxy. Besides possessing excellent mechanical and electrical properties, the HfO_2-epoxy dielectrics can be deposited at low temperatures (ca. 150 °C).[109]

For MOS capacitors, the erase speed can be drastically enhanced by embedding Au nanocrystals in the Al_2O_3/SiO_2 matrix where the ALD-deposited Al_2O_3 serves as control oxide.[110] Very recently, F. Medjdoub et al. have shown that ALD can be used to deposit a thin film of Al_2O_3 in order to improve the leakage characteristics of a MOSHEMT device.[111]

Choi et al.[112] have shown that iridium oxide (IrO_2) nanodots can be deposited by PEALD and embedded in SiO_2 gate dielectrics to act as discrete charge traps in next generation charge-trap flash-memory devices.

9. Conclusions and an Outlook

Atomic Layer Deposition is now a mature technique which has demonstrated its unique ability for processing of ultrathin overlayers on complex-shaped substrates. ALD is already the method-of-choice in the semiconductor industry for depositing only few nanometer thick highly insulating oxide films and with precursor and process design other major applications will follow soon. This technology has also become an attractive coating technique for the developments of nanostructured materials with optimized chemical or physical properties driven by fundamental research. E. g. the conformal coating of semiconductor nanowires and carbon nanotubes and optimization of 3D photonic crystal are currently very active research areas. The ALD also allows for the synthesis of nanostructured materials and objects with a high degree of precision in chemical composition and doping concen-

ADVANCED MATERIALS

tration. The developments of low-temperature deposition processes (< 100 °C) have significantly enlarged the application range of ALD and the method was already applied on temperature-sensitive materials, like biomolecules and polymer nanostructures. ALD of polymer films has recently been demonstrated for polyimides[113] and the process development will most probably be extended to other organic coatings in near future. Another specific feature of ALD, besides the capability of conformal deposition on non-planar surfaces, is a certain degree of selectivity for depositions on patterned surfaces, which gives additional opportunities for nanostructured materials synthesis. In addition to the booming activities on the depositions of high-*k* dielectrics for the semiconductor industry, the application of ALD in combination with nanostructured materials for conventional optics, solar cells, fuel cells, nanoparticle coatings and jewellery is intensively under discussion and in some cases has already reached the commercial stage.

Received: January 10, 2007
Revised: May 31, 2007
Published online: October 2, 2007

[1] T. Suntola, J. Antson, *US Patent 4 058 430*, **1977**.
[2] L. Niinistö, *Ann. Chim.* **1997**, *87*, 221.
[3] M. Leskelä, M. Ritala, *Angew. Chem. Int. Ed.* **2003**, *42*, 5548.
[4] L. Niinistö, J. Päiväsaari, J. Niinistö, M. Putkonen, M. Nieminen, *Phys. Status Solidi A* **2004**, *201*, 1443.
[5] H. Kim, P. C. McIntyre, *J. Korean Phys. Soc.* **2006**, *48*, 5.
[6] R. Puurunen, *J. Appl. Phys.* **2005**, *97*, 121 301.
[7] H. Kim, *J. Vac. Sci. Technol. B* **2003**, *21*, 2231.
[8] M. Leskelä, M. Kemell, K. Kukli, V. Pore, E. Santala, M. Ritala, J. Lu, *Mater. Sci. Eng. C* **2007**, *27*, 1504.
[9] International Technology Road Map for Semiconductors, http://public.itrs.net/ (accessed September 2007).
[10] C. Düsco, N. Q. Khanh, Z. Horvath, I. Barsony, M. Utriainen, S. Lehto, M. Nieminen, L. Niinistö, *J. Electrochem. Soc.* **1996**, *143*, 683.
[11] R. G. Gordon, D. Hausmann, E. Kim, J. Shepard, *Chem. Vap. Deposition* **2003**, *9*, 73.
[12] J. E. Herrera, J. H. Kwak, J. Z. Hu, Y. Wang, C. H. F. Peden, *Top. Catal.* **2006**, *39*, 245.
[13] J. W. Elam, D. Routkevich, P. P. Mardilovich, S. M. George, *Chem. Mater.* **2003**, *15*, 3507.
[14] S. O. Kucheyev, J. Biener, Y. M. Wang, T. F. Baumann, K. J. Wu, T. van Buuren, A. V. Hamza, J. H. Satcher, Jr., J. W. Elam, M. J. Pellin, *Appl. Phys. Lett.* **2005**, *86*, 083 108.
[15] T. F. Baumann, J. Biener, Y. M. Wang, S. O. Kucheyev, E. J. Nelson, J. H. Satcher, J. W. Elam, M. J. Pellin, A. V. Hamza, *Chem. Mater.* **2006**, *18*, 6106.
[16] J. Biener, T. F. Baumann, Y. M. Wang, E. J. Nelson, S. O. Kucheyev, A. V. Hamza, M. Kemell, M. Ritala, M. Leskelä, *Nanotechnology* **2007**, *18*, 055 303.
[17] M. S. Sander, M. J. Cote, W. Gu, B. M. Kile, C. P. Tripp, *Adv. Mater.* **2004**, *16*, 2052.
[18] C. J. Yang, S.-M. Wang, S.-W. Liang, Y.-H. Chang, C. Chen, *Appl. Phys. Lett.* **2007**, *90*, 033 104.
[19] L. K. Tan, A. S. M. Chong, X. S. E. Tang, H. Gao, *J. Phys. Chem. C* **2007**, *111*, 4964.
[20] M. Kemell, V. Pore, J. Tupala, M. Ritala, M. Leskelä, *Chem. Mater.* **2007**, *19*, 1816.
[21] H. Shin, J. K. Jeong, J. Lee, M. M. Sung, J. Kim, *Adv. Mater.* **2004**, *16*, 1197.
[22] M. Rooth, A. Johansson, M. Boman, A. Hårsta, *Mater. Res. Soc. Symp. Proc.* **2006**, *901*, Ra24–05.1.
[23] B. S. Lim, A. Rahtu, R. G. Gordon, *Nat. Mater.* **2003**, *2*, 749.
[24] A. Johansson, T. Törndahl, L. M. Ottosson, M. Boman, J.-O. Carlsson, *Mater. Sci. Eng. C* **2003**, *23*, 823.
[25] M. Utriainen, M. Kröger-Laukkanen, L.-S. Johansson, L. Niinistö, *Appl. Surf. Sci.* **2000**, *137*, 151.
[26] M. Daub, M. Knez, U. Gösele, K. Nielsch, *J. Appl. Phys.* **2007**, *101*, 09J111.
[27] Z. Li, R. G. Gordon, *Chem. Vap. Deposition* **2006**, *12*, 435.
[28] P. Cheng, T. Mitsui, D. P. Farmer, J. Golovchenko, R. G. Gordon, D. Branton, *Nano Lett.* **2004**, *4*, 1333.
[29] H. J. Fan, P. Werner, M. Zacharias, *Small* **2006**, *2*, 700.
[30] M. T. Björk, B. J. Ohlsson, T. Sass, A. I. Persson, C. Thelander, M. H. Magnusson, K. Deppert, L. R. Wallenberg, L. Samuelson, *Nano Lett.* **2002**, *2*, 87.
[31] R. Solanki, J. Huo, J. L. Freeouf, B. Miner, *Appl. Phys. Lett.* **2002**, *81*, 3864.
[32] G. Kipshidze, B. Yavich, A. Chandolu, J. Yon, V. Kuryatkov, I. Ahmad, D. Aurongzeb, M. Holz, H. Temkin, *Appl. Phys. Lett.* **2005**, *86*, 033 104.
[33] D. Zhang, S. Moore, J. Wei, A. Alkhateeb, D. Gangadean, H. Mahmood, J. Lantrips, D. N. McIlroy, A. D. LaLonde, M. G. Norton, J. S. Young, C. Wang, *Appl. Phys. Lett.* **2005**, *86*, 263 110.
[34] C. F. Hermann, F. H. Fabreguette, D. S. Finch, R. Geiss, S. M. George, *Appl. Phys. Lett.* **2005**, *87*, 123 110.
[35] D. B. Farmer, R. G. Gordon, *Nano Lett.* **2006**, *6*, 699.
[36] Y. S. Min, E. J. Bae, K. S. Jeong, Y. J. Cho, J. H. Lee. W. B. Choi, G. S. Park, *Adv. Mater.* **2003**, *15*, 1019.
[37] D. B. Farmer, R. G. Gordon, *Electrochem. Solid-State Lett.* **2005**, *8*, G89.
[38] D. Wang, Y. L. Chang, Q. Wang, J. Cao, D. B. Farmer, R. G. Gordon, H. Dai, *J. Am. Chem. Soc.* **2004**, *126*, 11 602.
[39] a) H. J. Fan, M. Knez, R. Scholz, K. Nielsch, E. Pippel, D. Hesse, M. Zacharias, U. Gösele, *Nat. Mater.* **2006**, *5*, 627. b) H. J. Fan, M. Knez, R. Scholz, D. Hesse, K. Nielsch, M. Zacharias, U. Gösele, *Nano Lett.* **2007**, *7*, 993.
[40] H. J. Fan, M. Knez, R. Scholz, K. Nielsch, E. Pippel, D. Hesse, U. Gösele, M. Zacharias, *Nanotechnology* **2006**, *17*, 5157.
[41] B. Min, J. S. Lee, J. W. Hwang, K. H. Keem, M. I. Kang, K. Cho, M. Y. Sung, S. Kim, M.-S. Lee, S. O. Park, J. T. Moon, *J. Cryst. Growth* **2003**, *252*, 565.
[42] M. Law, L. E. Greene, A. Radenovic, T. Kuykendall, J. Liphardt, P. Yang, *J. Phys. Chem. B* **2006**, *110*, 22 652.
[43] J. F. Conley, L. Strecker, Y. Ono, *Appl. Phys. Lett.* **2005**, *87*, 223 114.
[44] T. Nishida, N. Kobayashi, T. Ban, *Appl. Phys. Lett.* **2002**, *82*, 1.
[45] M. Kang, J.-S. Lee, S.-K. Sim, B. Min, K. Cho, H. Kim, M.-Y. Sung, S. Kim, S. A. Song, M.-S. Lee, *Thin Solid Films* **2004**, *466*, 265.
[46] M. J. Biercuk, D. J. Monsma, C. M. Marcus, J. S. Becker, R. G. Gordon, *Appl. Phys. Lett.* **2003**, *83*, 2405.
[47] K. S. Park, E. K. Seo, Y. R. Do, K. Kim, M. M. Sung, *J. Am. Chem. Soc.* **2006**, *128*, 858.
[48] E. K. Seo, J. W. Lee, S. M. Hyung, M. M. Sung, *Chem. Mater.* **2004**, *16*, 1878.
[49] K. J. Park, J. M. Doub, T. Gougousi, G. N. Parsons, *Appl. Phys. Lett.* **2005**, *86*, 051 903.
[50] J. P. Lee, M. M. Sung, *J. Am. Chem. Soc.* **2004**, *126*, 28.
[51] R. Chen, H. Kim, P. C. McIntyre, D. W. Porter, S. F. Bent, *Appl. Phys. Lett.* **2005**, *86*, 191 910.
[52] R. Chen, S. F. Bent, *Adv. Mater.* **2006**, *18*, 1086.
[53] A. V. Whitney, J. W. Elam, S. Zou, A. V. Zinovev, P. C. Stair, G. C. Schatz, R. P. van Duyne, *J. Phys. Chem. B* **2005**, *109*, 20 522.
[54] X. D. Wang, E. Graugnard, J. S. King, Z. L. Wang, C. J. Summers, *Nano Lett.* **2004**, *4*, 2223.
[55] E. Graugnard, J. S. King, D. P. Gaillot, C. J. Summers, *Adv. Funct. Mater.* **2006**, *16*, 1187.
[56] C. A. Wilson, R. K. Grubbs, S. M. George, *Chem. Mater.* **2005**, *17*, 5625.

[57] X. Liang, L. F. Hakim, G.-D. Zhan, J. A. McCormick, S. M. George, A. W. Winter, *J. Am. Ceram. Soc.* **2007**, *90*, 57.
[58] W. Gasser, Y. Uchida, M. Matsumura, *Thin Solid Films* **1994**, *250*, 213.
[59] J. W. Klaus, O. Sneh, S. M. George, *Science* **1997**, *278*, 1934.
[60] Y. Luo, D. Slater, M. Han, J. Moryl, R. M. Osgood, *Appl. Phys. Lett.* **1997**, *71*, 3799.
[61] M. D. Groner, F. H. Fabreguette, J. W. Elam, S. M. George, *Chem. Mater.* **2004**, *16*, 639.
[62] J. D. Ferguson, A. W. Weimer, S. M. George, *Chem. Mater.* **2004**, *16*, 5602.
[63] R. H. A. Ras, M. Kemell, J. De Wit, M. Ritala, G. Ten Brinke, M. Leskelä, O. Ikkala, *Adv. Mater.* **2007**, *19*, 102.
[64] Q. Peng, X.-Y. Sun, J. C. Spagnola, G. K. Hyde, R. J. Spontak, G. N. Parsons, *Nano Lett.* **2007**, *7*, 719.
[65] M. Knez, A. Kadri, C. Wege, U. Gösele, H. Jeske, K. Nielsch, *Nano Lett.* **2006**, *6*, 1172.
[66] J. Huang, X. Wang, Z. L. Wang, *Nano Lett.* **2006**, *6*, 2325.
[67] M. Kemell, V. Pore, M. Ritala, M. Leskelä, M. Linden, *J. Am. Chem. Soc.* **2005**, *127*, 14 178.
[68] J. W. Klaus, S. M. George, *Surf. Sci.* **2000**, *447*, 81.
[69] J. S. King, E. Graungnard, O. M. Roche, D. N. Sharp, J. Scrimgeour, R. G. Denning, A. J. Turberfield, C. J. Summers, *Adv. Mater.* **2006**, *18*, 1561.
[70] M. Putkonen, L. Niinistö, *Thin Solid Films* **2006**, *514*, 145.
[71] J. Keränen, C. Guimon, E. Iiskola, A. Auroux, L. Niinistö, *J. Phys. Chem. B* **2003**, *107*, 10 773.
[72] Y. Lu, S. Bangsaruntip, X. Wang, L. Zhang, Y. Nishi, H. Dai, *J. Am. Chem. Soc.* **2006**, *128*, 3518.
[73] M. Scharrer, X. Wu, A. Yamilov, H. Cao, R. P. H. Chang, *Appl. Phys. Lett.* **2005**, *86*, 151 113.
[74] G. A. Ten Eyck, S. Pimanpang, H. Bakhru, T. M. Lu, G. C. Wang, *Chem. Vap. Deposition* **2006**, *12*, 290.
[75] G. A. Ten Eyck, J. J. Senkevich, F. Tang, D. Liu, S. Pimanpang, T. Karaback, G. C. Wang, T. M. Lu, C. Jezewski, W. A. Lanford, *Chem. Vap. Deposition* **2005**, *11*, 60.
[76] A. Birner, R. B. Wehrspohn, U. Gösele, K. Busch, *Adv. Mater.* **2001**, *13*, 377.
[77] S. Matthias, F. Müller, C. Jamois, R. B. Wehrspohn, U. Gösele, *Adv. Mater.* **2004**, *16*, 2166.
[78] P. V. Braun, S. A. Rinne, F. Garvia-Santamaria, *Adv. Mater.* **2006**, *18*, 2665.
[79] H. M. Yates, M. E. Pemble, H. Miguez, A. Blanco, C. Lopez, F. Meseguer, L. Vazquez, *J. Cryst. Growth* **1998**, *193*, 9.
[80] A. Blanco, E. Chomski, S. Grabtchak, M. Ibisate, S. John, S. W. Leonard, C. Lopez, F. Meseguer, H. Miguez, J. P. Mondia, G. A. Ozin, O. Toader, H. M. van Driel, *Nature* **2000**, *405*, 437.
[81] F. G. Fleming, S. Y. Lin, I. El-Kady, R. Biswas, K. M. Ho, *Nature* **2002**, *417*, 52.
[82] N. Tétreault, G. von Freymann, M. Deubel, M. Hermatschweiler, F. Pérez-Willard, S. John, M. Wegener, G. A. Ozin, *Adv. Mater.* **2006**, *18*, 457.
[83] A. Rugge, J. S. Becker, R. G. Gordon, S. H. Tolbert, *Nano Lett.* **2003**, *3*, 1293.
[84] J. S. King, C. W. Neff, C. J. Summers, W. Park, S. Blomquist, E. Forsythe, D. Morton, *Appl. Phys. Lett.* **2003**, *83*, 2566.
[85] J. S. King, C. W. Neff, S. Blomquist, E. Forsythe, D. Morton, C. J. Summers, *Phys. Status Solidi B* **2004**, *241*, 763.
[86] J. S. King, E. Graungnard, C. J. Summers, *Adv. Mater.* **2005**, *17*, 1010.
[87] A. Rugge, J. S. Park, R. G. Gordon, S. H. Tolbert, *J. Phys. Chem. B* **2005**, *109*, 3765.
[88] M. Scharrer, A. Yamilov, X. Wu, H. Cao, R. P. H. Chang, *Appl. Phys. Lett.* **2006**, *88*, 201 103.
[89] I. M. Povey, D. Whitehead, K. Thomas, M. E. Pemble, M. Bardosova, J. Renard, *Appl. Phys. Lett.* **2006**, *89*, 104 103.
[90] Z. A. Sechrist, B. T. Schwartz, J. H. Lee, J. A. McCormick, R. Piestum, W. Park, S. M. George, *Chem. Mater.* **2006**, *18*, 3562.
[91] J. S. King, E. Graugnard, C. J. Summers, *Appl. Phys. Lett.* **2006**, *88*, 081 109.
[92] X. Wang, C. Neff, E. Graungnard, Y. Ding, J. S. King, L. A. Pranger, R. Tannenbaum, Z. L. Wang, C. J. Summers, *Adv. Mater.* **2005**, *17*, 2103.
[93] R. M. Costescu, D. G. Cahill, F. H. Fabreguette, Z. A. Sechrist, S. M. George, *Science* **2004**, *303*, 989.
[94] Z. A. Sechrist, F. H. Fabreguette, O. Heintz, T. M. Phung, D. C. Johnson, S. M. George, *Chem. Mater.* **2005**, *17*, 3475.
[95] J. J. Wang, X. Deng, R. Varghese, A. Nikolov, P. Sciortino, F. Liu, L. Chen, X. Liu, *J. Vac. Sci. Technol. B* **2005**, *23*, 3209.
[96] J. J. Wang, A. Nikolov, Q. Wu, *IEEE Photonics Technol. Lett.* **2006**, *18*, 2650.
[97] A. Javey, H. Kim, M. Brink, Q. Wang, A. Ural, J. Guo, P. McIntyre, P. McEuen, M. Lundstrom, H. Dai, *Nat. Mater.* **2002**, *1*, 241.
[98] A. Javey, J. Guo, D. B. Farmer, Q.Wang, E. Yenilmez, R. G. Gordon, M. Lundstrom, H. Dai, *Nano Lett.* **2004**, *4*, 1319.
[99] K. Keem, D.-Y. Jeong, S. Kim, M.-S. Lee, I.-S. Yeo, U.-I. Shung, J.-T. Moon, *Nano Lett.* **2006**, *6*, 1451.
[100] M. Nanu, J. Schoonman, A. Gossens, *Adv. Mater.* **2004**, *16*, 453.
[101] G. Stampfer, T. Helbling, D. Obergfell, B. Schöberle, M. K. Tripp, A. Jungen, S. Roth, V. M. Bright, C. Hierold, *Nano Lett.* **2006**, *6*, 233.
[102] K. K. Yadawalli, N. R. Anderson, T. A. Orlova, A. O. Orlov, G. L. Snider, J. Elam, *J. Vac. Sci. Technol. B* **2004**, *22*, 3119.
[103] S. Samanta, Z. Y. L. Tan, W. J. Woo, G. Samudra, S. Lee, L. K. Bera, N. Balasubramanian, *J. Vac. Sci. Technol. B* **2005**, *23*, 2278.
[104] W. K. Kim, W. H. Nam, S. H. Kim, S. H. Rhee, *J. Chem. Eng. Jpn.* **2005**, *38*, 578.
[105] M. Ritala, K. Kukli, A. Rahtu, P. I. Räisänen, M. Leskelä, T. Sajavaara, J. Keinonen, *Science* **2000**, *288*, 319.
[106] D.Wang, Q. Wang, A. Javey, R. Tu, H. Dai, H. Kim, P. C. McIntyre, T. Krisnamohan, K. C. Saraswat, *Appl. Phys. Lett.* **2003**, *83*, 2432.
[107] D. Wang, H. Dai, *Appl. Phys. A* **2006**, *85*, 217.
[108] T. W. Scharf, S. V. Prasad, M. T. Dugger, P. G. Kotula, R. S. Goeke, R. K. Grubbs, *Acta Mater.* **2006**, *54*, 4731.
[109] Q. Cao, M.-G. Xia, M. Shim, J. A. Rogers, *Adv. Funct. Mater.* **2006**, *16*, 2355.
[110] C.-C. Wang, Y.-K. Chiou, C.-H. Chang, J.-Y. Tseng, C.-Y. Chen, T.-B. Wu, *J. Phys. D* **2007**, *40*, 1673.
[111] F. Medjdoub, N. Sarazin, M. Tordjman, M. Magis, M. A. di Forte-Poisson, M. Knez, E. Delos, C. Gaquiere, S. L. Delage, E. Kohn, *IEEE Electron. Device Lett.* **2007**, *43*, 691.
[112] S. Soi, Y.-K. Cha, B.-S. Seo, S. Park, J.-H. Park, S. Shin, K. S. Seol, J.-B. Park, Y.-Park, Y. Park, I.-K. Yoo, S. H. Choi, *J. Phys. D* **2007**, *40*, 1426.
[113] M. Putkonen, J. Harjuoja, T. Sajavaara, L. Niinistö, *J. Mater. Chem.* **2007**, *17*, 664.